HHS Public Access

Author manuscript

Mol Pharm. Author manuscript; available in PMC 2019 May 20.

Published in final edited form as:

Mol Pharm. 2018 May 07; 15(5): 1778–1790. doi:10.1021/acs.molpharmaceut.7b01024.

Improvement in Therapeutic Efficacy and Reduction in Cellular Toxicity: Introduction of a Novel Anti-PSMA-Conjugated Hybrid Antiandrogen Nanoparticle

Chellappagounder Thangavel[*,†], **Maryna Perepelyuk**[‡,▽], **Ettickan Boopathi**[§,▽], **Yi Liu**[†], **Steven Polischak**[§], **Deepak A. Deshpande**[§], **Khadija Rafiq**[§], **Adam P. Dicker**[†,‖], **Karen E. Knudsen**[†,⊥,#], **Sunday A. Shoyele**[‡], and **Robert B. Den**[*,†,⊥,#]

[†]Department of Radiation Oncology, Sidney Kimmel Medical College, Thomas Jefferson University, Philadelphia, Pennsylvania 19107, United States

[§]Department of Medicine, Center for Translational Medicine, Sidney Kimmel Medical College, Thomas Jefferson University, Philadelphia, Pennsylvania 19107, United States

[⊥]Department of Cancer Biology, Sidney Kimmel Medical College, Thomas Jefferson University, Philadelphia, Pennsylvania 19107, United States

[#]Department of Urology, Sidney Kimmel Medical College, Thomas Jefferson University, Philadelphia, Pennsylvania 19107, United States

[‡]Department of Pharmaceutical Science, College of Pharmacy, Thomas Jefferson University, Philadelphia, Pennsylvania 19107, United States

[‖]Department of Pharmacology and Experimental Therapeutics, Thomas Jefferson University, Philadelphia, Pennsylvania 19107, United States

Abstract

Second generation antiandrogens have improved overall survival for men with metastatic castrate resistant prostate cancer; however, the antiandrogens result in suppression of androgen receptor (AR) activity in all tissues resulting in dose limiting toxicity. We sought to overcome this limitation through encapsulation in a prostate specific membrane antigen (PSMA)–conjugated nanoparticle. We designed and characterized a novel nanoparticle containing an antiandrogen, enzalutamide. Selectivity and enhanced efficacy was achieved through coating the particle with PSMA. The PSMA-conjugated nanoparticle was internalized selectively in AR expressing prostate cancer cells. It did not elicit an inflammatory effect. The efficacy of enzalutamide was not

[*]**Corresponding Authors**: Thangavel Chellappagounder, Ph.D., Department of Radiation Oncology, Sidney Kimmel Cancer Center, Sidney Kimmel Medical College at Thomas Jefferson University, 111 South 11th Street, Philadelphia, PA 19107- 5097, United States; Phone: (215) 955-8579; Fax: (215) 955-0412; thangavel.chellappagounder@jefferson.edu., Robert B. Den, M.D., Department of Radiation Oncology, Urology & Cancer Biology, Sidney Kimmel Cancer Center, Sidney Kimmel Medical College at Thomas Jefferson University, 111 South 11th Street, Philadelphia, PA 19107-5097, United States: Phone: (215) 955-0284; Fax: (215) 955-0412; robert.den@jefferson.edu.

[▽]**Author Contributions** M.P. and E.B. contributed equally to this study. Conception and design: C.T., S.A.S., K.E.K, and R.B.D. Reagents/material contribution: K.R., S.P., and D.A.D. Development of methodology: C.T., Y.L., E.B., S.P., D.A.D., S.A.S., K.E.K., and R.B.D. Acquisition of data: C.T., M.P., Y.L., E.B., and R.B.D. Analysis and interpretation of data (e.g., statistical analysis, biostatistics): C.T., E.B., and R.B.D. Writing, review, and/or revision of the manuscript: C.T., K.E.K., A.P.D., R.B.D. Study supervision: C.T., S.A.S., and R.B.D.

The authors declare the following competing financial interest(s): S.S. holds a patent on the hybrid nanoparticle.

compromised through insertion into the nanoparticle; in fact, lower systemic drug concentrations of enzalutamide resulted in comparable clinical activity. Normal muscle cells were not impacted by the PSMA-conjugated containing antiandrogen. This approach represents a novel strategy to increase the specificity and effectiveness of antiandrogen treatment for men with castrate resistant prostate cancer. The ability to deliver higher drug concentrations in prostate cancer cells may translate into improved clinical end points including overall survival.

Graphical Abstract

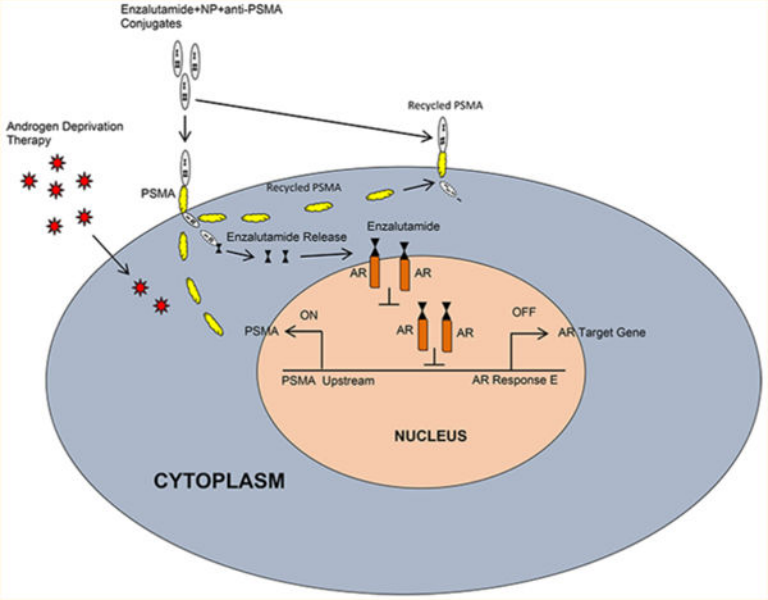

Keywords

prostate specific antigen; prostate specific membrane antigen; hybrid nanoparticle; prostate cancer; androgen receptor; enzalutamide

INTRODUCTION

Since Huggins' and Hodges'[1] seminal discovery that castration led to prostate glandular atrophy, surgical or medical castration has been a central component for the treatment for men with advanced prostate cancer. Mechanistically, androgen deprivation therapy (ADT) decreases androgen signaling either by downregulating androgen synthesis or through antagonistic binding to the receptor, leading to reduced AR transcriptional activity. While initially effective, cells adapt, leading to formation of castrate resistance (CRPC) and ultimately death from prostate cancer.[2]

Over the past 5 years, there have been several significant advancements in management of men with CRPC.[3] Specifically, novel agents, which inhibit AR signaling and block androgen synthesis, have led to improvements in overall survival for men with castrate resistant disease.[4] These drugs demonstrated that targeting the AR is critical even in the setting of CRPC. Nevertheless, CRPC remains an incurable disease despite these advances.

One approach for enhancing therapy is to deliver higher intratumoral concentrations of antiandrogens. Studies of antiandrogen therapy demonstrate a dose–response relationship, with higher concentrations of drugs leading to increased levels of cellular apoptosis.[5,6] However, this has been tempered due to increased systemic side effects[7] resulting from aberration of normal tissue in AR-dependent cellular function. These toxicities can result in decreased quality of life[8] and result in premature halting of a life prolonging therapy.[9] Further, despite the high response rate with ADT, resistance and adverse effects are universal. Side effects from treatment include increased risk for metabolic syndrome, osteoporosis, diabetes, cardiovascular disease, and neurocognitive decline.[10,11] Further, the psychological effects and sexual dysfunction impacts not only men undergoing treatment but also partners.[12]

Herein, we describe the utilization of a novel approach using nanoparticles to selectively and specifically deliver antiandrogens to prostate cancer cells. Our approach is unique in that it overcomes several challenges in nanomedicine including (a) substantial uptake of nanoparticles by the mononuclear phagocyte system (MPS), leading to short blood circulation time; (b) inability to invoke an endosomal escape once internalization by host cells has occurred; and (c) the elicitation of immunotoxicity.[13,14] Our study demonstrates that this novel delivery method can enhance therapeutic efficacy and can kill tumors while sparing normal tissue function.

MATERIALS AND METHODS

Cell Culture.

LNCaP, LAPC4, PC3, MCF7, H9C2, HASM, and C2C12 were maintained in improved minimum essential medium (IMEM), HA'S F-12, and DMEM supplemented with 10% FBS (heat-inactivated FBS) and maintained at 37 °C in a humidified 5% CO2 incubator.

Chemicals and Reagents.

Human IgG was purchased from Equitech Bio (TX, U.S.A.). Poloxamer-188, RNase-free water, and fetal bovine albumin (FBS) were obtained from Fisher Scientific. Enzalutamide and monoclonal mouse anti-PSMA from Selleckchem and Millipore were used.

Preparation of Enzalutamide-Loaded Hybrid Nano-particles.

Hybrid nanoparticles were prepared based on our previously reported protocol.[15] A mass of 50 mg of excipient-free human IgG was dissolved in 0.01 N HCl containing 20 mg of poloxamer-188 and 1 mg of enzalutamide in 1 mL with 10 mg of sodium tripoliphosphate as a carrier to make 10 mL of total solution in a 50 mL beaker. The final concentration of human IgG in each solution amounted to 5 mg/mL. This solution was then slowly titrated with 0.01 N NaOH to bring the pH of the mixture to 7, which is the isoelectric point (pI) of human IgG as determined in our laboratory using isoelectric focusing. The nanoparticles were continuously mixed on a magnetic stirrer for additional 10 min. At the pI, enzalutamide-loaded hybrid nanoparticles were spontaneously precipitated. The colloidal suspension was then centrifuged with a microcentrifuge (Eppendorf Centrifuge 5418) at 2000 rpm for 5 min. The nanoparticles were rinsed with double distilled deionized water

before being redispersed in water and snapfrozen using liquid nitrogen. This was then loaded into a freezedryer (Labconco FreezeZone 4.6), and lyophilization was performed for 48 h.

Thiolation of Anti-PSMA-mAb.

Thiolation of anti-PSMA-mAb was performed as described.[15,16] Briefly, 1.3×10^{-4} M of Traut's reagent (2-iminothiolane·HCl) was prepared in phosphate buffered saline (pH 7.4). A volume of 500 μL of this solution was then added to 1 mL of 1.3×10^{-6} M (0.2 mg/ mL) of anti-PSMA-mAb solution. The reaction was stirred for 2 h at 25 °C. The mixture was then centrifuged at 4000 rpm and 10 °C for 15 min using 30 kDa cutoff centrifugal ultrafilters (Millipore Corp) to exclude unreacted Traut's reagent.

Activation of Hybrid Nanoparticles with Heterobifunctional Cross-Linker.

A solution of 5 mg/mL of hybrid nanoparticles in 0.1 M phosphate buffer (pH 7.2) was added to 2 mg/mL of *N*-[*p*-maleimidophenyl] isocyanate (PMPI), a heterobifunctional cross-linker that links sulfhydryl to hydroxyl groups. PMPI was dissolved in 50 mM phosphate buffer (pH 8.0). The reaction was incubated for 3 h at room temperature, after which the activated nanoparticles were centrifuged at 4000 rpm at 10 °C for 15 min using 30 kDa ultrafilters (Millipore Corp.).

Preparation of Anti-PSMA mAb Functionalized Hybrid Nanoparticles.

Specific mouse monoclonal antibody to prostate specific membrane antigen (PSMA) was purchased from Millipore (Billerica, MA, U.S.A.). PSMA antibody specificity was checked by immunofluorescence in PSMA proficient (LNCaP) and deficient (PC3) prostate cancer cell lines. PSMA antibody was thiolated.[15,17] Thiolated anti-PSMA- mAb and activated hybrid nanoparticles from the above reactions were covalently linked together in the next procedure. Preparation of anti-PSMA mAb functionalized hybrid nanoparticles was carried out as described.[15,17] The activated nanoparticles were finally functionalized with the thiolated anti-PSMA-mAb by adding 500 μL of 2 mg/mL thiolated anti-PSMA-mAb to 4 mL of activated nanoparticle suspension (5 mg/mL) and then incubated for 3 h at 25 °C. The functionalized nanoparticles were centrifuged for 30 min at 4000 rpm and 10 °C. Unconjugated anti-PSMA-mAb in the supernatant was quantified using the Total Protein Kit (Micro Lowry, Sigma) based on the supplier's instructions.

Hybrid Nanoparticle Characterization (HPC).

Characterization of hybrid nanoparticle was carried out as described.[17] Photon correlation spectroscopy (PCS) using a ZetaSizer Nano ZS (Malvern Instruments, U.K.) was used to measure the particle size and zeta potential of the nanoparticles. Pellets were redispersed in deionized water and sonicated for approximately 5 min. Intensity autocorrelation was measured at a scattering angle (θ) of 173°. The *Z*-average and polydispersity index (PDI) were recorded in triplicate. For zeta potential, samples were taken in a universal dip cell (Malvern Instruments), and the zeta potential was recorded in triplicate.

The morphology of the nanoparticles was imaged by scanning electron microscopy (SEM). Suspensions of nanoparticles were dropped on an aluminum stub and allowed to dry at room

temperature. Samples were then coated with a thin layer of palladium. Coated samples were imaged using a Zeiss Supra 50 V system (Carl Zeiss Meditec AG, Jena, Germany).

Drug Treatments and Flow Cytometry Analysis.

Cell proliferation was assessed via BrdU incorporation by flow cytometry analysis as described previously.[18,19] LNCaP, LAPC4, PC3, or MCF7 cells were exposed to vehicle, enzalutamide, hybrid nanoparticle-loaded enzalutamide, hybrid nanoparticle, hybrid nanoparticle-conjugated anti-PSMA, or enzalutamide-loaded hybrid nanoparticles conjugated with anti-PSMA. The cells were pulse-labeled with BrdU for 2 h prior to harvest. Cells were fixed in 75% ethanol, pelleted, resuspended in 2 N HCl + 0.5 mg/mL pepsin, and incubated at room temperature for 30 min. Sodium tetraborate (0.1 mol/L) was added to neutralize 2 N HCl. The cell pellets were washed with IFA buffer, centrifuged, and then washed with IFA + 0.5% Tween 20 solution. The pellet was resuspended in IFA solution containing FITC-conjugated anti-BrdU antibody (BD Bioscience), incubated in the dark at room temperature for 45 min, washed with IFA + 0.5% Tween-20, and pelleted. The pellet was then suspended in PBS containing propidium iodide (0.2 μg/μL) and analyzed for BrdU incorporation using a Beckman Coulter Cell Lab Quanta SC flow cytometer. Flow cytometry analysis was performed using FlowJo software (GE Healthcare, Piscataway, NJ, U.S.A.).

Cell Growth Analysis.

LNCaP or LAPC4 cells were exposed to vehicle, enzalutamide, hybrid nanoparticle-loaded enzalutamide, hybrid nanoparticle, hybrid nanoparticle-conjugated anti-PSMA, or enzalutamide-loaded hybrid nanoparticles conjugated with anti-PSMA. Viable cells were counted from 0, 2, 4, 6, and 8 days after post drug treatment, and a quantitative analysis was carried out using Prism Graph Pad v.7.0.

Immunofluorescence and Confocal Microscopy.

Actively growing LNCaP or PC3 cells exposed to vehicle, enzalutamide, nanoparticles, nanoparticle-conjugated enzalutamide, enzalutamide-loaded hybrid nanoparticle anti-PSMA conjugates, or FITC-loaded hybrid nanoparticles at indicated times were fixed with 4% formaldehyde, permeabilized with 0.1% triton X-100 for 5 min and blocked with 1% BSA for 1 h. Vehicle treated cells were probed with mouse monoclonal PSMA primary antibody for 1 h at 37 °C and washed three times with PBS and probed mouse FITC for 45 min at RT and washed thrice with PBS and mounted with antifade mount with DAPI. Cells exposed to enzalutamide-loaded hybrid nanoparticle anti-PSMA conjugates were fixed with 4% formaldehyde, permeabilized with 0.1% Triton X-100 for 5 min, and blocked with 1% BSA for 1 h and probed mouse FITC for 45 min at room temperature and were washed thrice with PBS and mounted with an antifade mount with DAPI. Cells exposed to FITC-conjugated anti-PSMA were washed thrice and directly mounted with an antifade mount with DAPI. The stained cells were imaged using NIKON confocal microscopy (Thomas Jefferson University, Facility).

Toxicity and Immunofluorescence.

NCaP, PC3, H9C2, HASM, or C2C12 cells were exposed to vehicle or various concentrations of enzalutamide (0, 0.5, 1, and 5 μM) or nanoparticle (NP) or enzalutamide-loaded hybrid nanoparticle-conjugated anti-PSMA or vehicle or enzalutamide alone or FITC alone or FITC-loaded hybrid nanoparticles conjugated with anti-PSMA for 0, 0.5, 1, 3, or 24 h or 2, 4, or 6 days in culture and stained for phalloidin (F-actin) as described[20] or PSMA or FITC and DAPI nuclear stain. Alternatively, hybrid nanoparticles and LPS were injected in to nude mice and toxicity was tested by measuring TNF-alpha using ELISA in the blood serum by the indicated time points. The stained slides were imaged using confocal microscopy at Thomas Jefferson University, Philadelphia.

RNA Analysis.

Total RNA was isolated from LNCaP, MCF7, or PC3 cells exposed to vehicle, enzalutamide, hybrid nanoparticle-loaded enzalutamide, hybrid nanoparticle, hybrid nanoparticle-conjugated anti-PSMA, or enzalutamide-loaded hybrid nanoparticles conjugated with anti-PSMA. Total RNA was reverse transcribed and subjected to semiquantitative PCR or real time PCR. Real time PCR was performed with an ABI Step-One apparatus using the Power SYBR Green Master Mix. Target mRNA primers for AR target KLK3 and GAPDH were used as previously described.[20–24] The signals were normalized with an internal control GAPDH and quantitated by ΔΔCT.

RESULTS

Enzalutamide Side Effects on Nontarget Cells.

The second-generation nonsteroidal antiandrogen drug, enzalutamide, is an oral inhibitor that inhibits androgen receptor (AR) dimerization and DNA binding, inhibits androgen receptor nuclear translocation, and impinges on coactivator recruitment and transcription.[25] As expected, introduction of enzalutamide inhibits cell cycle in AR-positive hormone sensitive LNCaP cells (Figure 1A, left), but failed to abrogate S-phase in AR-negative PC3 cells (Figure 1A, right). Common side effects of enzalutamide include fatigue, musculoskeletal pain, diarrhea, hot flashes, and headaches.[26] The androgen and AR signaling pathway is necessary for developing skeletal muscle and maintaining muscle mass, strength, and protein synthesis.[27] To determine the impact of enzalutamide, we examined the effects on several muscle cells including H9C2 (cardiac myoblasts), HASM (human airway smooth muscle), and C2C12 (muscle myoblast) cells. Increasing concentrations of enzalutamide exposure significantly decreased the F-actin bundles (Figure 1B,C), as measured by phalloidin staining in all cell models, indicating that AR antagonism alters muscle cytoskeletal structure. Given the AR role in muscle growth and selection of muscle fiber type,[28] this may account for the musculoskeletal symptoms noted clinically, impressing the importance for tumor-selective targeting of AR function.

Development of Enzalutamide-Encapsulated Hybrid Nanoparticle–Anti-PSMA Conjugates.

Nanoparticle-encapsulated targeted drug delivery enables minimization of systemic exposure and subsequently toxicity.[29] To ensure that our hybrid nanoparticles maintain long blood

circulation time, avoid endosomal escape following internalization, and do not evoke immunotoxicity, our nanoparticle incorporates human immunoglobulin G (human IgG) and biodegradable poloxamer-188 (Polyoxyethylene-polyoxypropylene block copolymer) (Figure 2A), for efficient and targeted delivery of payload of drugs to tumors.[15,17,30] Poloxamer-188 functions as a stealth polymer by preventing macrophage uptake of nanoparticles bypassing the reticuloendothelial system (RES) and reducing opsonization by serum proteins.[31] To achieve prostate cancer specificity, prostate-specific membrane antigen (PSMA), a classic type-II membrane glycoprotein, was chosen (Figure 2B,C). PSMA has ideal characteristics as an enzyme-biomarker target due to its specific expression in prostate cancer cells[32] and its internalization upon binding targeting ligands.[33] Transmission electron microscopy demonstrated the size of the hybrid nanoparticle to be approximately 200 nm (Figure 2D). Anti-PSMA conjugates of enzalutamide–hybrid nano-particles were tested for their release in physiological pH 7.5 and cellular pH 5.0, and it was demonstrated that maximal enzalutamide release from nanoparticle occurs at cellular physiological pH 5.0 (Figure 2E). Enzalutamide (MDV3100) encapsulation efficiency and loading capacity were calculated (Tables 1 and 2).

Safety and Nontoxicity of Anti-PSMA Conjugates of Enzalutamide–Hybrid Nanoparticles.

Different organ derived normal muscle cells were exposed to vehicle, MDV3100, nanoparticle (NP), nanoparticle conjugates of MDV3100, nanoparticle conjugates of anti-PSMA, or anti-PSMA conjugates of enzalutamide–hybrid nanoparticles for 6 days in culture. Cells exposed to MDV3100 alone and nanoparticle conjugates of MDV3110 demonstrated toxic effects: decreased F-actin expression and poor cytoskeleton organization (Figure 3A,B) as compared to vehicle, nanoparticle, anti-PSMA-conjugated nanoparticle, and anti-PSMA conjugates of enzalutamide–hybrid nanoparticles (Figure 3A,B). Injection of the nanoparticles into nude mice failed to elicit an increase in serum levels of TNF-alpha in contrast to LPS (Figure 3C,D).

Enzalutamide Internalizes in PSMA Specific Cells.

To confirm that enzalutamide-loaded–anti-PSMA hybrid nanoparticles internalize specifically in cancer cells, as mediated via PSMA, nanoparticles were exposed to AR-positive and -negative cells. AR-positive LNCaP cells express PSMA on the cell surface in contrast to AR-negative PC3 cells (Figure 4A, left panel), and PSMA expression increased with increasing concentrations of enzalutamide-loaded–anti-PSMA hybrid nanoparticle conjugates (right panel) at 24 h in LNCaP cells. Further, anti-PSMA nanoparticles internalized over 24 h as measured using immunofluorescence in LNCaP cells but failed to internalize into PC3 cells as measured through anti-PSMA localization (Figure 4B). Enzalutamide-encapsulated nanoparticle-conjugated anti-PSMA had increased internalization via PSMA over time (Figure 4C, FITC load mimics enzalutamide payload).

Inhibition of AR Signaling and Prostate Cancer Growth by Enzalutamide-Encapsulated Hybrid Nanoparticle–Anti-PSMA Conjugates.

Next, we interrogated whether internalized PSMA-conjugated nanoparticles released enzalutamide, leading to halting of AR signaling and cell cycle arrest. For this experiment, clinically achievable dosing of enzalutamide was utilized as control. Enzalutamide treatment

reduces prostate cancer cell growth and leads to down-regulation of AR target genes.[7] We noted that encapsulation in the nanoparticle did not interfere with the ability of enzalutamide to halt cell cycle or reduce expression of the AR target gene, PSA, in AR-positive LNCaP or MCF7 cells (Figure 5A,B,D,E), whereas the drug had no impact on PC3 cells (Figure 5C,F, right panel).

Production of a Maximal Therapeutic Response in Prostate Cancer by a Single Minimal Dose (SMD) of an Enzalutamide-Encapsulated Hybrid Nanoparticle–Anti-PSMA Conjugate.

Clinical efficacy of oral or injectable enzalutamide can be limited by its very short-lived half-life in blood and may require a high dosage or additional dose of enzalutamide to suppress cancer growth. In order to limit the plasma concentration of enzalutamide and thus minimize systemic toxicity, we sought to examine if lower concentrations of drug encapsulated in the nanoparticle could result in comparable AR suppression and cell cycle inhibition. We used a FITC payload (FITC payload mimics MDV3100 payload) to measure the stability of the nanoparticle and noted that encapsulation translated into higher and more sustained fluorescent signal for up to 6 days (Figure 6A). Next, we noted that lower concentrations of encapsulated enzalutamide (1 μM) had improved cell cycle inhibition in two AR-positive cell lines (Figure 6B,C). Further, this suppression of cell cycle was greater than that of the higher concentration of enzalutamide alone as compared to Figure 5A. This reduction in cell cycle translated into diminished cell growth (Figure 6D,E). These results demonstrate that the enzalutamide-encapsulated hybrid anti-PSMA nanoparticle can deliver a clinically efficacious dose with longer stability and less systemic toxicity.

The schematic (Figure 7) illustrates that androgen deprivation therapy (ADT) increases PSMA expression and the molecular sequence of events with introduction of the enzalutamide-encapsulated hybrid nanoparticle–anti-PSMA conjugate to prostate cancer cells. The nanoparticles are internalized via PSMA. Through the internalization process, enzalutamide is released within the cell at an acidic pH. The internalized PSMA molecules are then constitutively recycled to the cell surface. Enzalutamide binds with the androgen receptor and inhibits the natural ligand (DHT) binding. Enzalutamide binding prevents dimerization and nuclear translocation of AR. Inactive AR fails to associate on AREs, inhibiting the transcription of AR target genes, resulting in inhibition of cell cycle and growth.

DISCUSSION

The androgen receptor (AR) is expressed in multiple tissues including normal prostate, liver, muscle, bone, thyroid, and brain.[34] A member of the superfamily of ligand-activated transcription factors, AR possesses three crucial domains: transactivation, ligand binding, and DNA binding.[35] AR is a component of a multiprotein complex with heat-shock protein and immunophilins, and upon ligand binding, it dissociates, recruits coactivators, and translocates from the cytoplasm to the nucleus.[36] AR signaling predominates through binding to the promoter of androgen responsive genes. Enzalutamide directly antagonizes AR ligand binding resulting in blockage of AR signaling pathways.[37] Within the context of prostate cancer, this results in improved overall survival.[38,39]

Half of all men diagnosed with prostate cancer receive androgen receptor directed therapy during their overall cancer care.[40] Current management strategies include systemic reduction of circulating androgens, reduction in peripheral androgen production, or direct antagonism of AR function. While successful, these approaches result in substantial toxicity and detriment of quality of life.

We sought to reduce toxicity through encapsulation of an antiandrogen in a PSMA-conjugated nanoparticle. PSMA, prostate-specific membrane antigen, is only expressed on prostate epithelium, duodenal mucosa, and a subset of the proximal renal tubules[41] and thus has been an attractive biomarker for prostate cancer specificity. PSMA is nearly universally expressed in the hormone sensitive setting of the disease, and PSMA expression is increased in the setting of androgen deprivation therapy. However, it has been noted to be heterogeneously expressed in the castrate resistant setting even within a single patient[42,43] when measured by circulating tumor cells or metastases. Further, the late stage variant, neuroendocrine prostate cancer, is characterized by a lack of expression of androgen receptor and subsequent targets including PSMA.[44] Notwithstanding this heterogeneity, the early success of using PSMA-labeled radionuclides including alpha particles[45,46] in management of men with castrate resistant prostate cancer suggest that a PSMA targeted approach warrants further clinical investigation.

In our study, we modeled alteration in normal tissue using multiple muscle cells. The androgen receptor signaling pathway is critical in increasing muscle mass and strength by inducing fiber hypertrophy.[47,48] This is primarily driven through increased protein synthesis[49] with a concomitant decrease in protein breakdown.[50] Clinically, patients note loss of muscle weakness, fatigue, as well as musculoskeletal pain.[51] Encapsulation of enzalutamide in a PSMA-conjugated nanoparticle resulted in sparing of muscle fiber function. Further, the nanoparticle did not elicit an immune response as measured by serum TNF-alpha levels.

Nanoparticles possess several advantages as compared to conventional drug preparations including improved bioavailability, increasing half-life for clearance, and drug targeting to specific sites of action.[52] In our study, we noted specificity, as the nanoparticle loaded with enzalutamide only had an impact on AR-positive, PSMA-expressing cells. MCF7 cells express low levels of AR;[53] thus, when exposed to enzalutamide, there was reduction in both BrdU and KLK3 expression. Unexpectedly, we found that encapsulation of enzalutamide in the PSMA conjugate did not completely abrogate the impact of enzalutamide on BrdU and KLK3 expression in MCF7 cells. We hypothesize that this may be due to the ability of MCF7 cells to acidify their extracellular milieu by a dual mechanism,[54] given that drug release from the nanoparticle is pH-dependent (Figure 2E). However, this is not a major issue in the context of prostate cancer.

An additional benefit of the nanoparticle encapsulation, is increased sensitivity, as we were able to reduce the dosing of enzalutamide while maintaining efficacy. This should translate into improved efficacy and mitigate formation of castrate resistance through overexpression of the androgen receptor. The higher localized cancer-specific concentration and lower systemic exposure of drug yields many benefits including lower systemic drug exposure.

From a patient's perspective, this should result in decreased drug-related side effects and the potential to safely deliver doses that were heretofore considered systemically toxic.

ACKNOWLEDGMENTS

The study was supported by a Young Investigator Award from the Prostate Cancer Foundation (to R.B.D.), a Physician Research Training Award from the Department of Defense Grant (PC101841 to R.B.D.), Grant #IRG 08-060-04 from the American Cancer Society, a PA Cure Award (to K.E.K.), NIH grants (R01 CA099996 to K.E.K.), (R01 DK100483 to E.B.), (RO1 HL11278 to K.R.), and a PCF Challenge Award (to K.E.K.). The authors thank members of the K. Knudsen laboratory for input and comment.

ABBREVIATIONS

ADT	androgen deprivation therapy
AR	androgen receptor
CRPC	castrate resistant prostate cancer
DMEM	Dulbecco's Modified Eagle Medium
FBS	fetal bovine serum
FITC	fluorescein isothiocyanate
GCP II	glutamate carboxypeptidase II
KLK3	kallikrein-3
IgG	immunoglobulin
PCS	photon correlation spectroscopy
PDI	polydispersity index
PSA	prostate specific antigen
PSMA	prostate specific membrane antigen
RES	reticuloendothelial system
SEM	scanning electron microscope
TNF	tumor necrosis factor

REFERENCES

(1). Huggins C; Hodges CV Studies on prostatic cancer. I. The effect of castration, of estrogen and of androgen injection on serum phosphatases in metastatic carcinoma of the prostate. J. Urol 2002, 167 (2), 948–951; Discussion 952. Reprinted by J. Urol. With permission from Cancer Res, 1941, 1, 293–297.10.1016/S0022-5347(02)80307-X [PubMed: 11905923]

(2). Siegel RL; Miller KD; Jemal A Cancer statistics, 2016. Ca-Cancer J. Clin 2016, 66 (1), 7–30. [PubMed: 26742998]

(3). Seisen T; Roupret M; Gomez F; Malouf GG; Shariat SF; Peyronnet B; Spano JP; Cancel-Tassin G; Cussenot O A comprehensive review of genomic landscape, biomarkers and treatment

sequencing in castration-resistant prostate cancer. Cancer Treat. Rev 2016, 48, 25–33. [PubMed: 27327958]

(4). Roviello G; Sigala S; Sandhu S; Bonetta A; Cappelletti MR; Zanotti L; Bottini A; Sternberg CN; Fox SB; Generali D Role of the novel generation of androgen receptor pathway targeted agents in the management of castration-resistant prostate cancer: A literature based meta-analysis of randomized trials. Eur. J. Cancer 2016, 61, 111–21. [PubMed: 27162152]

(5). Clegg NJ; Wongvipat J; Joseph JD; Tran C; Ouk S; Dilhas A; Chen Y; Grillot K; Bischoff ED; Cai L; Aparicio A; Dorow S; Arora V; Shao G; Qian J; Zhao H; Yang G; Cao C; Sensintaffar J; Wasielewska T; Herbert MR; Bonnefous C; Darimont B; Scher HI; Smith-Jones P; Klang M; Smith ND; De Stanchina E; Wu N; Ouerfelli O; Rix PJ; Heyman RA; Jung ME; Sawyers CL; Hager JH ARN-509: a novel antiandrogen for prostate cancer treatment. Cancer Res 2012, 72 (6), 1494–503. [PubMed: 22266222]

(6). Tran C; Ouk S; Clegg NJ; Chen Y; Watson PA; Arora V; Wongvipat J; Smith-Jones PM; Yoo D; Kwon A; Wasielewska T; Welsbie D; Chen CD; Higano CS; Beer TM; Hung DT; Scher HI; Jung ME; Sawyers CL Development of a secondgeneration antiandrogen for treatment of advanced prostate cancer. Science 2009, 324 (5928), 787–90. [PubMed: 19359544]

(7). Scher HI; Beer TM; Higano CS; Anand A; Taplin ME; Efstathiou E; Rathkopf D; Shelkey J; Yu EY; Alumkal J; Hung D; Hirmand M; Seely L; Morris MJ; Danila DC; Humm J; Larson S; Fleisher M; Sawyers CL Prostate Cancer Foundation/Department of Defense Prostate Cancer Clinical Trials, C. Antitumour activity of MDV3100 in castration-resistant prostate cancer: a phase 1–2 study. Lancet 2010, 375 (9724), 1437–46. [PubMed: 20398925]

(8). Dacal K; Sereika SM; Greenspan SL Quality of life in prostate cancer patients taking androgen deprivation therapy. J. Am. Geriatr. Soc 2006, 54 (1), 85–90. [PubMed: 16420202]

(9). Steigler A; Mameghan H; Lamb D; Joseph D; Matthews J; Franklin I; Turner S; Spry N; Poulsen M; North J; Kovacev O; Denham J A quality assurance audit: phase III trial of maximal androgen deprivation in prostate cancer (TROG 96.01). Australas. Radiol 2000, 44 (1), 65–71. [PubMed: 10761262]

(10). Nead KT; Gaskin G; Chester C; Swisher-McClure S; Dudley JT; Leeper NJ; Shah NH Androgen Deprivation Therapy and Future Alzheimer's Disease Risk. J. Clin. Oncol 2016, 34 (6), 566–71. [PubMed: 26644522]

(11). Nguyen PL; Alibhai SM; Basaria S; D'Amico AV; Kantoff PW; Keating NL; Penson DF; Rosario DJ; Tombal B; Smith MR Adverse effects of androgen deprivation therapy and strategies to mitigate them. Eur. Urol 2015, 67 (5), 825–36. [PubMed: 25097095]

(12). Donovan KA; Walker LM; Wassersug RJ; Thompson LM; Robinson JW Psychological effects of androgen-deprivation therapy on men with prostate cancer and their partners. Cancer 2015, 121 (24), 4286–99. [PubMed: 26372364]

(13). Aigner A Applications of RNA interference: current state and prospects for siRNA-based strategies in vivo. Appl. Microbiol. Biotechnol 2007, 76 (1), 9–21. [PubMed: 17457539]

(14). Jagani HV; Josyula VR; Palanimuthu VR; Hariharapura RC; Gang SS Improvement of therapeutic efficacy of PLGA nanoformulation of siRNA targeting anti-apoptotic Bcl-2 through chitosan coating. Eur. J. Pharm. Sci 2013, 48 (4–5), 611–8. [PubMed: 23291045]

(15). Perepelyuk M; Thangavel C; Liu Y; Den RB; Lu B; Snook AE; Shoyele SA Biodistribution and Pharmacokinetics Study of siRNA-loaded Anti-NTSR1-mAb-functionalized Novel Hybrid Nanoparticles in a Metastatic Orthotopic Murine Lung Cancer Model. Mol. Ther.–Nucleic Acids 2016, 5, e282. [PubMed: 26812654]

(16). Yousefpour P; Atyabi F; Vasheghani-Farahani E; Movahedi M; Dinarvand R Targeted delivery of doxorubicin-utilizing chitosan nanoparticles surface-functionalized with anti-Her2 trastuzumab. Int. J. Nanomed 2011, 6, 1977–1990.

(17). Dim N; Perepelyuk M; Gomes O; Thangavel C; Liu Y; Den R; Lakshmikuttyamma A; Shoyele SA Novel targeted siRNA-loaded hybrid nanoparticles: preparation, characterization and in vitro evaluation. J. Nanobiotechnol 2015, 13, 61.

(18). Balasubramaniam S; Comstock CE; Ertel A; Jeong KW; Stallcup MR; Addya S; McCue PA; Ostrander WF Jr.; Augello MA; Knudsen KE Aberrant BAF57 signaling facilitates prometastatic phenotypes. Clin. Cancer Res 2013, 19 (10), 2657–67. [PubMed: 23493350]

(19). Augello MA; Burd CJ; Birbe R; McNair C; Ertel A; Magee MS; Frigo DE; Wilder-Romans K; Shilkrut M; Han S; Jernigan DL; Dean JL; Fatatis A; McDonnell DP; Visakorpi T; Feng FY; Knudsen KE Convergence of oncogenic and hormone receptor pathways promotes metastatic phenotypes. J. Clin. Invest 2013, 123 (1), 493–508. [PubMed: 23257359]

(20). Thangavel C; Boopathi E; Liu Y; Haber A; Ertel A; Bhardwaj A; Addya S; Williams N; Ciment SJ; Cotzia P; Dean JL; Snook A; McNair C; Price M; Hernandez JR; Zhao SG; Birbe R; McCarthy JB; Turley EA; Pienta KJ; Feng FY; Dicker AP; Knudsen KE; Den RB RB Loss Promotes Prostate Cancer Metastasis. Cancer Res 2017, 77 (4), 982–995. [PubMed: 27923835]

(21). Thangavel C; Boopathi E; Ciment S; Liu Y; O'Neill R; Sharma A; McMahon SB; Mellert H; Addya S; Ertel A; Birbe R; Fortina P; Dicker AP; Knudsen KE; Den RB The retinoblastoma tumor suppressor modulates DNA repair and radio-responsiveness. Clin. Cancer Res 2014, 20 (21), 5468–5482. [PubMed: 25165096]

(22). Thangavel C; Dean JL; Ertel A; Knudsen KE; Aldaz CM; Witkiewicz AK; Clarke R; Knudsen ES Therapeutically activating RB: reestablishing cell cycle control in endocrine therapy-resistant breast cancer. Endocr.-Relat. Cancer 2011, 18 (3), 333–45.

(23). Wang X; Huang Y; Christie A; Bowden M; Lee GS; Kantoff PW; Sweeney CJ Cabozantinib Inhibits Abiraterone's Upregulation of IGFIR Phosphorylation and Enhances Its Anti-Prostate Cancer Activity. Clin. Cancer Res 2015, 21 (24), 5578–87. [PubMed: 26289068]

(24). Comstock CE; Augello MA; Benito RP; Karch J; Tran TH; Utama FE; Tindall EA; Wang Y; Burd CJ; Groh EM; Hoang HN; Giles GG; Severi G; Hayes VM; Henderson BE; Le Marchand L; Kolonel LN; Haiman CA; Baffa R; Gomella LG; Knudsen ES; Rui H; Henshall SM; Sutherland RL; Knudsen KE Cyclin D1 splice variants: polymorphism, risk, and isoform-specific regulation in prostate cancer. Clin. Cancer Res 2009, 15 (17), 5338–49. [PubMed: 19706803]

(25). Hoffman-Censits J; Kelly WK Enzalutamide: a novel antiandrogen for patients with castrate-resistant prostate cancer. Clin. Cancer Res 2013, 19 (6), 1335–9. [PubMed: 23300275]

(26). Cella D; Ivanescu C; Holmstrom S; Bui CN; Spalding J; Fizazi K Impact of enzalutamide on quality of life in men with metastatic castration-resistant prostate cancer after chemotherapy: additional analyses from the AFFIRM randomized clinical trial. Ann. Oncol 2015, 26 (1), 179–85. [PubMed: 25361992]

(27). Herbst KL; Bhasin S Testosterone action on skeletal muscle. Curr. Opin. Clin. Nutr. Metab. Care 2004, 7 (3), 271–7. [PubMed: 15075918]

(28). Ting HJ; Chang C Actin associated proteins function as androgen receptor coregulators: an implication of androgen receptor's roles in skeletal muscle. J. Steroid Biochem. Mol. Biol 2008, 111 (3–5), 157–63. [PubMed: 18590822]

(29). Choi G; Kwon OJ; Oh Y; Yun CO; Choy JH Inorganic nanovehicle targets tumor in an orthotopic breast cancer model. Sci. Rep 2015, 4, 4430.

(30). Lakshmikuttyamma A; Sun Y; Lu B; Undieh AS; Shoyele SA Stable and efficient transfection of siRNA for mutated KRAS silencing using novel hybrid nanoparticles. Mol. Pharmaceutics 2014, 11 (12), 4415–24.

(31). Jain D; Athawale R; Bajaj A; Shrikhande S; Goel PN; Gude RP Studies on stabilization mechanism and stealth effect of poloxamer 188 onto PLGA nanoparticles. Colloids Surf., B 2013, 109, 59–67.

(32). Pinto JT; Suffoletto BP; Berzin TM; Qiao CH; Lin S; Tong WP; May F; Mukherjee B; Heston WD Prostate-specific membrane antigen: a novel folate hydrolase in human prostatic carcinoma cells. Clin. Cancer Res 1996, 2 (9), 1445–1451. [PubMed: 9816319]

(33). Liu H; Rajasekaran AK; Moy P; Xia Y; Kim S; Navarro V; Rahmati R; Bander NH Constitutive and antibody-induced internalization of prostate-specific membrane antigen. Cancer Res 1998, 58 (18), 4055–4060. [PubMed: 9751609]

(34). Ruizeveld de Winter JA; Trapman J; Vermey M; Mulder E; Zegers ND; van der Kwast TH Androgen receptor expression in human tissues: an immunohistochemical study. J. Histochem. Cytochem 1991, 39 (7), 927–36. [PubMed: 1865110]

(35). Roy AK; Tyagi RK; Song CS; Lavrovsky Y; Ahn SC; Oh TS; Chatterjee B Androgen receptor: structural domains and functional dynamics after ligand-receptor interaction. Ann. N. Y. Acad. Sci 2001, 949, 44–57. [PubMed: 11795379]

(36). Augello MA; Den RB; Knudsen KE AR function in promoting metastatic prostate cancer. Cancer Metastasis Rev 2014, 33 (2–3), 399–411. [PubMed: 24425228]

(37). Knudsen KE; Kelly WK Outsmarting androgen receptor: creative approaches for targeting aberrant androgen signaling in advanced prostate cancer. Expert Rev. Endocrinol. Metab 2011, 6 (3), 483–493. [PubMed: 22389648]

(38). Beer TM; Armstrong AJ; Rathkopf DE; Loriot Y; Sternberg CN; Higano CS; Iversen P; Bhattacharya S; Carles J; Chowdhury S; Davis ID; de Bono JS; Evans CP; Fizazi K; Joshua AM; Kim CS; Kimura G; Mainwaring P; Mansbach H; Miller K; Noonberg SB; Perabo F; Phung D; Saad F; Scher HI; Taplin ME; Venner PM; Tombal B Investigators, P. Enzalutamide in metastatic prostate cancer before chemotherapy. N. Engl. J. Med 2014, 371 (5), 424–33. [PubMed: 24881730]

(39). Scher HI; Fizazi K; Saad F; Taplin ME; Sternberg CN; Miller K; de Wit R; Mulders P; Chi KN; Shore ND; Armstrong AJ; Flaig TW; Flechon A; Mainwaring P; Fleming M; Hainsworth JD; Hirmand M; Selby B; Seely L; de Bono JS Investigators, A. Increased survival with enzalutamide in prostate cancer after chemotherapy. N. Engl. J. Med 2012, 367 (13), 1187–97. [PubMed: 22894553]

(40). Gunner C; Gulamhusein A; Rosario DJ The modern role of androgen deprivation therapy in the management of localised and locally advanced prostate cancer. J. Clin Urol 2016, 9 (2_suppl), 24–29. [PubMed: 28344813]

(41). Maraj BH; Aldersley MA; Markham AF Prostate-specific membrane antigen expression in the duodenum: implications in coeliac disease and immunotherapy for prostate cancer. Lancet 1998, 351 (9115), 1559–60. [PubMed: 10326547]

(42). Morin F; Beauregard JM; Bergeron M; Nguile Makao M; Lacombe L; Fradet V; Fradet Y; Pouliot F Metabolic Imaging of Prostate Cancer Reveals Intrapatient Intermetastasis Response Heterogeneity to Systemic Therapy. Eur. Urol Focus 2017; In press.10.1016/j.euf.2017.02.007

(43). Gorges TM; Riethdorf S; von Ahsen O; Nastały YP; Rock K; Boede M; Peine S; Kuske A; Schmid E; Kneip C; Konig F; Rudolph M; Pantel K Heterogeneous PSMA expression on circulating tumor cells: a potential basis for stratification and monitoring of PSMA-directed therapies in prostate cancer. Oncotarget 2016, 7 (23), 34930–34941. [PubMed: 27145459]

(44). Parimi V; Goyal R; Poropatich K; Yang XJ Neuro-endocrine differentiation of prostate cancer: a review. Am. J. Clin Exp Urol 2014, 2 (4), 273–285. [PubMed: 25606573]

(45). Kratochwil C; Bruchertseifer F; Rathke H; Hohenfellner M; Giesel FL; Haberkorn U; Morgenstern A Targeted Alpha Therapy of mCRPC with (225)Actinium-PSMA-617: Swimmer-Plot analysis suggests efficacy regarding duration of tumor-control. J. Nucl. Med 2018; jnumed. 117.20353910.2967/jnumed.117.203539.

(46). Kratochwil C; Bruchertseifer F; Giesel FL; Weis M; Verburg FA; Mottaghy F; Kopka K; Apostolidis C; Haberkorn U; Morgenstern A 225Ac-PSMA-617 for PSMA-Targeted alpha-Radiation Therapy of Metastatic Castration-Resistant Prostate Cancer. J. Nucl. Med 2016, 57 (12), 1941–1944. [PubMed: 27390158]

(47). Snyder PJ; Peachey H; Hannoush P; Berlin JA; Loh L; Lenrow DA; Holmes JH; Dlewati A; Santanna J; Rosen CJ; Strom BL Effect of testosterone treatment on body composition and muscle strength in men over 65 years of age. J. Clin. Endocrinol. Metab 1999, 84 (8), 2647–53. [PubMed: 10443654]

(48). Bhasin S; Storer TW; Berman N; Callegari C; Clevenger B ; Phillips J; Bunnell TJ; Tricker R; Shirazi A; Casaburi R The effects of supraphysiologic doses of testosterone on muscle size and strength in normal men. N. Engl. J. Med 1996, 335 (1), 1–7. [PubMed: 8637535]

(49). Ferrando AA; Tipton KD; Doyle D; Phillips SM; Cortiella J; Wolfe RR Testosterone injection stimulates net protein synthesis but not tissue amino acid transport. Am. J. Physiol 1998, 275 (5), E864–71. [PubMed: 9815007]

(50). Ferrando AA; Sheffield-Moore M; Yeckel CW; Gilkison B ; Jiang J; Achacosa A; Lieberman SA; Tipton K; Wolfe RR; Urban RJ Testosterone administration to older men improves muscle function: molecular and physiological mechanisms. Am. J. Physiol Endocrinol Metab 2002, 282 (3), E601–7. [PubMed: 11832363]

(51). Luo J; Graff JN Impact of enzalutamide on patient-related outcomes in metastatic castration-resistant prostate cancer: current perspectives. Res. Rep. Urol 2016, 8, 217–224. [PubMed: 27942507]

(52). Huang Y; Fan CQ; Dong H; Wang SM; Yang XC; Yang SM Current applications and future prospects of nanomaterials in tumor therapy. Int. J. Nanomed 2017, 12, 1815–1825.

(53). Cochrane DR; Bernales S; Jacobsen BM; Cittelly DM; Howe EN; D'Amato NC; Spoelstra NS; Edgerton SM; Jean A; Guerrero J; Gomez F; Medicherla S; Alfaro IE; McCullagh E; Jedlicka P; Torkko KC; Thor AD; Elias AD; Protter AA; Richer JK Role of the androgen receptor in breast cancer and preclinical analysis of enzalutamide. Breast Cancer Res 2014, 16 (1), R7. [PubMed: 24451109]

(54). Montcourrier P; Silver I; Farnoud R; Bird I; Rochefort H Breast cancer cells have a high capacity to acidify extracellular milieu by a dual mechanism. Clin. Exp. Metastasis 1997, 15 (4), 382–92. [PubMed: 9219726]

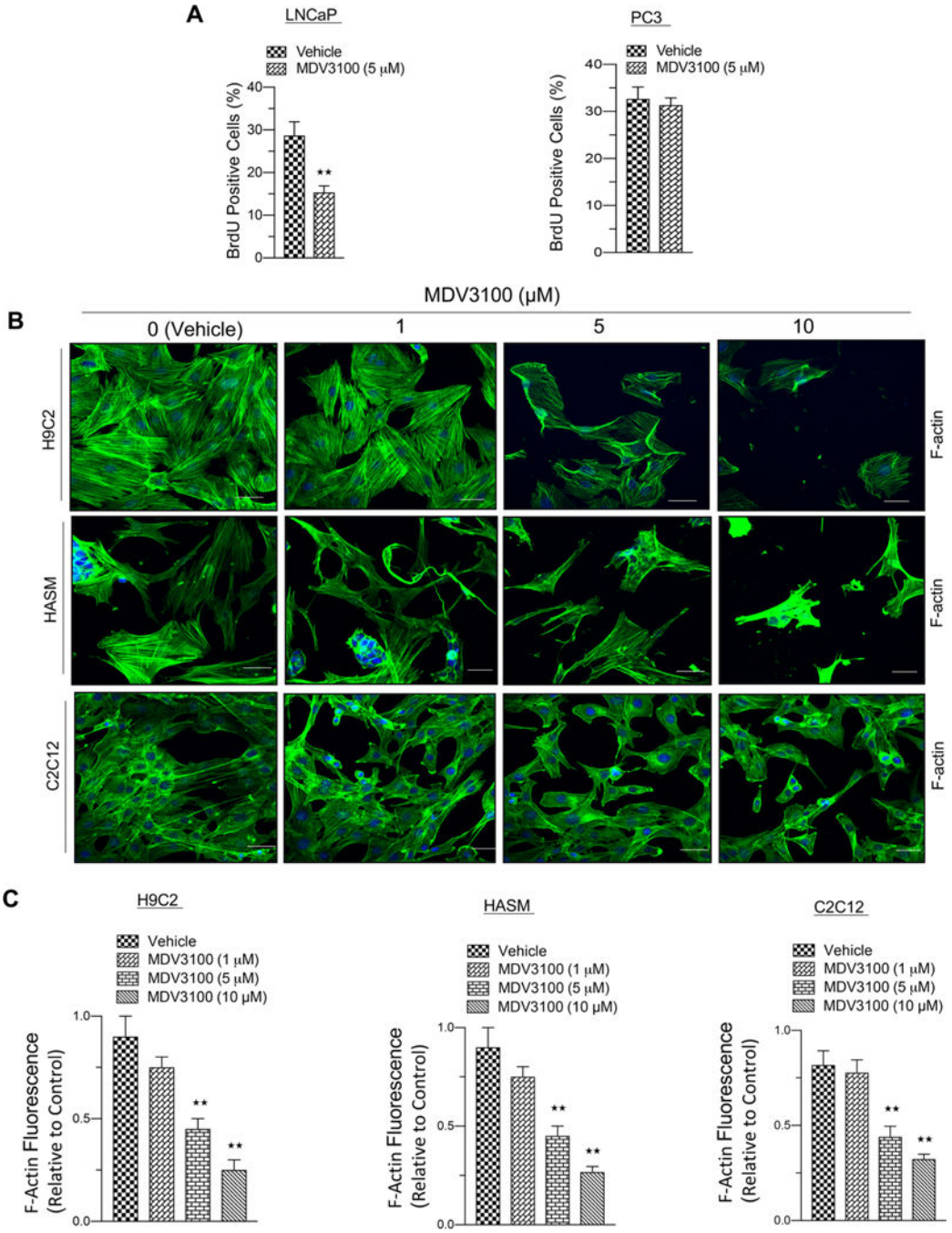

Figure 1.

Enzalutamide inhibits cell cycle in target cells and causes toxicity in nontarget cells. (A) Graphic representation of BrdU analysis in AR proficient (LNCaP) and AR deficient (PC3) prostate cancer cell lines in response to vehicle or enzalutamide treatment (5 μM). (B) Confocal microscopic images of F-actin staining from rat heart myoblast cells (H9C2), human airway smooth muscle cells (HASM), and mouse skeletal muscle cells (C2C12) in response to increasing concentrations of enzalutamide (0, 1, 5, and 10 μM) exposed for 2 days in culture. (C) Graphic representation of F-actin fluorescence from rat heart myoblast,

human airway smooth muscle, and mouse skeletal muscle cells in response to increasing concentrations of enzalutamide (vehicle, 1, 5, and 10 μM) exposed for 2 days in culture. Each data point is a mean ± SD from three or more independent experiments. $^{\star\star}p < 0.05$ were considered as statistically significant. Scale bar "–" = 20 μm.

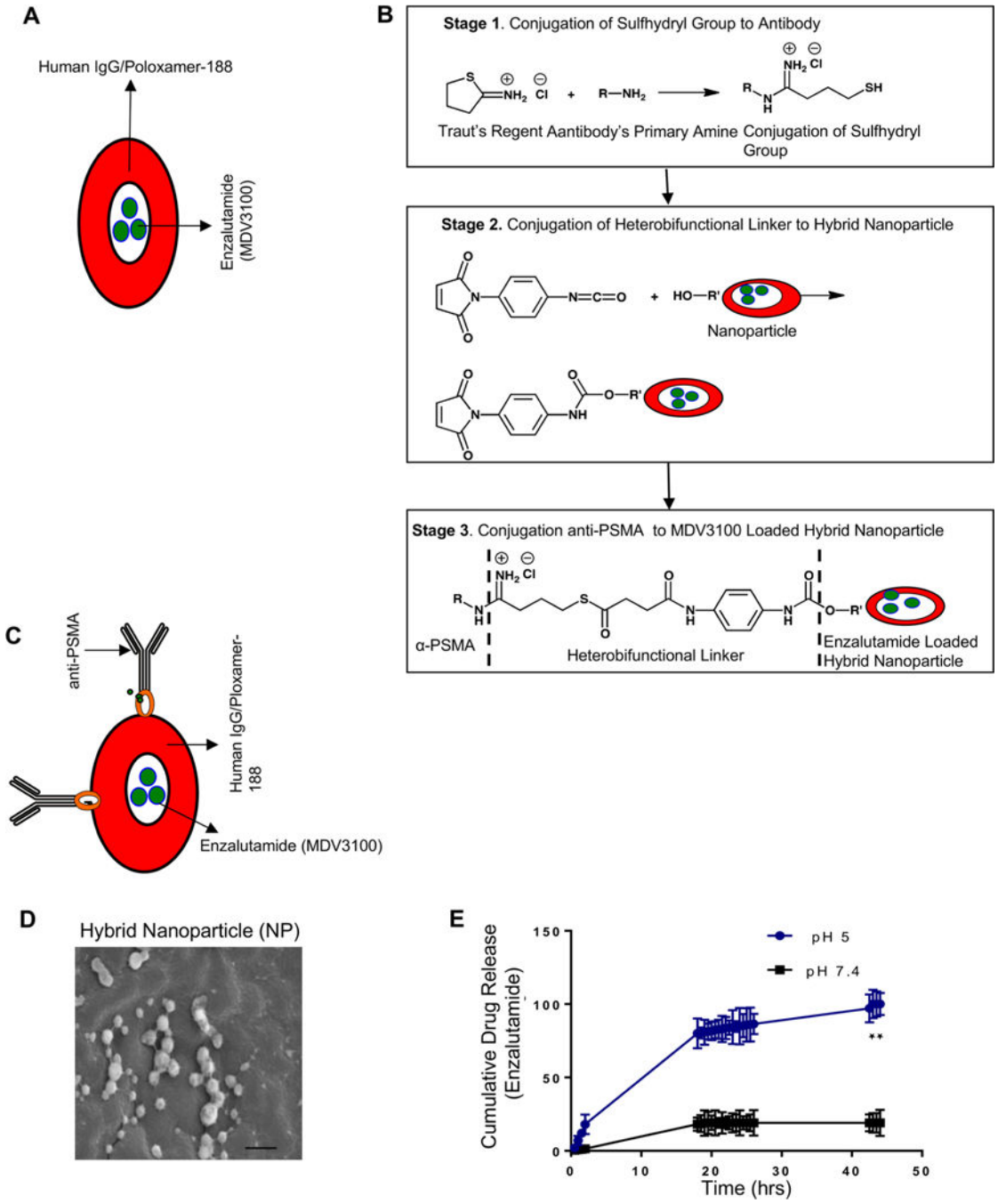

Figure 2.

Design and construction of enzalutamide-encapsulated–anti-PSMA-conjugated hybrid nanoparticle. (A) A schematic illustrates the embedding of enzalutamide to human IgG with an ecofriendly biopolymer ploxamer-188. (B) Schematics describe the conjugation of the sulfhydryl group to anti-PSMA (top panel), and the middle panels illustrate the conjugation of a heterobifunctional linker to hybrid nanoparticle, and the bottom panels describe the conjugation of α-PSMA to an MDV3100-loaded hybrid nanoparticle. (C) A cartoon summarizes the organization of the enzalutamide-loaded hybrid nanoparticle and NH_2 group

conjugation to anti-PSMA mAb. (D) Transmission electron microscopic picture of a hybrid nanoparticle with a size of "–" = 200 nm. (E) pH-dependent enzalutamide release from hybrid nanoparticle (cellular pH 5.0). Each data point is a mean ± SD from three or more independent experiments. $^{\star\star}p < 0.05$ were considered as statistically significant.

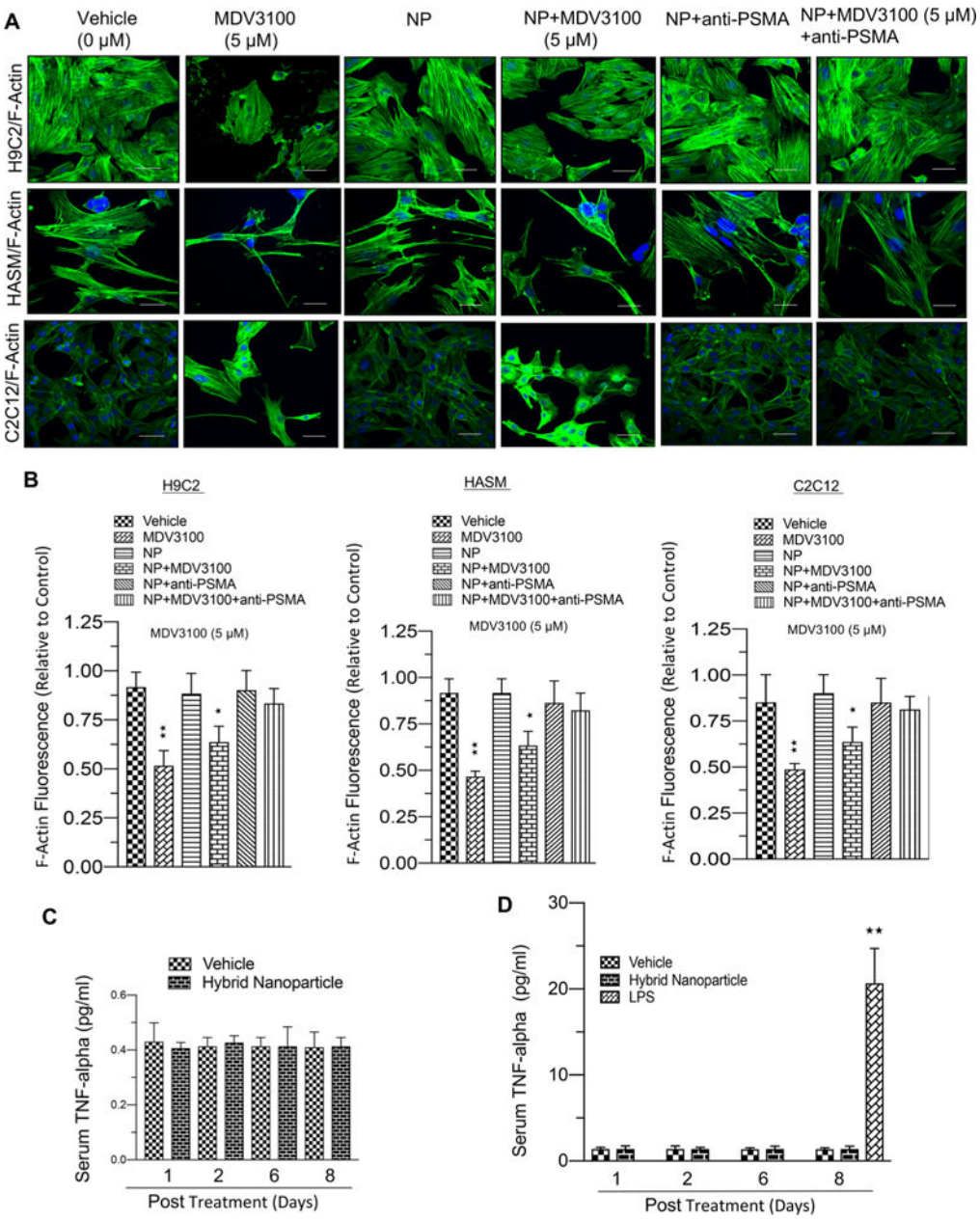

Figure 3.

Ecofriendly nature of enzalutamide-loaded–anti-PSMA-conjugated hybrid nanoparticle to nontarget cells. (A) F-actin stained confocal microscopic images from H9C2, HASM, and C2C12 cells exposed to vehicle, MDV3100 (5 μM), NP, NP+MDV (5 μM), NP+anti-PSMA, or enzalutamide-loaded–anti-PSMA-conjugated hybrid nanoparticle (5 μM) for 6 days in culture. (B) A graphic representation of F-actin fluorescence in H9C2, HASM, and C2C12 cells exposed to vehicle or MDV3100 (5 μM), NP, NP+MDV (5 μM), NP+anti-PSMA, or enzalutamide-loaded–anti-PSMA-conjugated hybrid nanoparticle (5 μM) for 6 days in culture. (C) A graphical representation of TNF-alpha levels in mouse blood serum in response to hybrid nanoparticle exposure. (D) A graphical representation of TNF-alpha levels in nude mouse blood serum in response to LPS exposure. Each data point is a mean ±

SD from three or more independent experiments and five or more animals. ★★$p < 0.05$ was considered as statistically significant. Scale bar "–" = 20 μm.

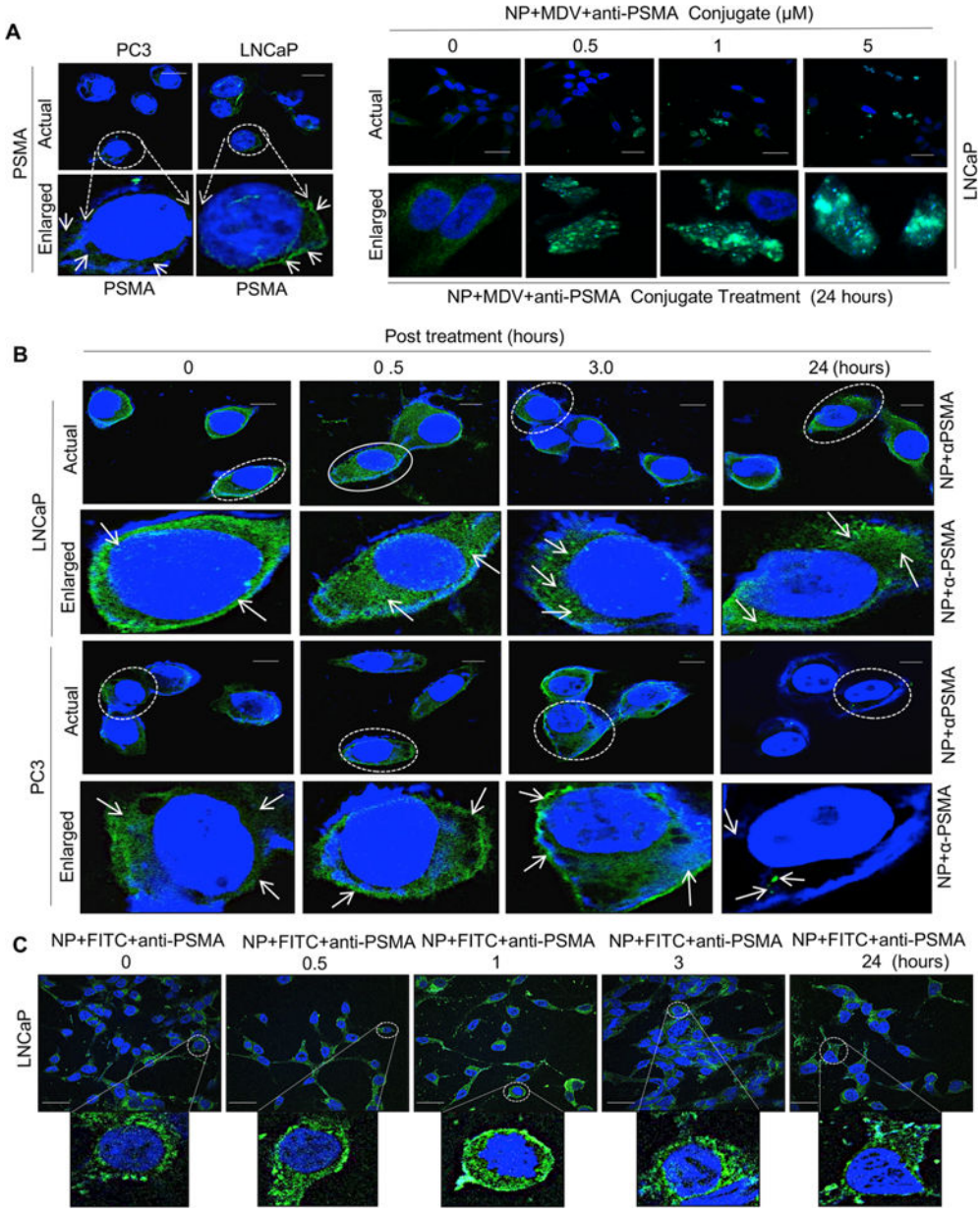

Figure 4.

PSMA specific internalization of hybrid nanoparticle in prostate cancer cells. (A) Immunolocalization of prostate specific membrane antigen (PSMA) in PSMA proficient and PSMA deficient prostate cancer isogenic LNCaP and PC3 models (left panel) and expression of PSMA in LNCaP cells in response to varying doses of hybrid nanoparticle-loaded enzalutamide–anti-PSMSA conjugates with indicated concentrations (right panel). (B) Confocal microscopic images of anti-PSMA internalization via PSMA in PSMA proficient and deficient LNCaP and PC3 isogenic PCa lines with indicated time points. (C) Confocal microscopic images of FITC in FITC-loaded (FITC load mimics MDV3100 payload) hybrid nanoparticle–anti-PSMA conjugates in LNCaP cells with indicated time

points. Each data point is a mean ± SD from three or more independent experiments. $^{\star\star}p < 0.05$ was considered as statistically significant. Scale bar "–" = 20 μm.

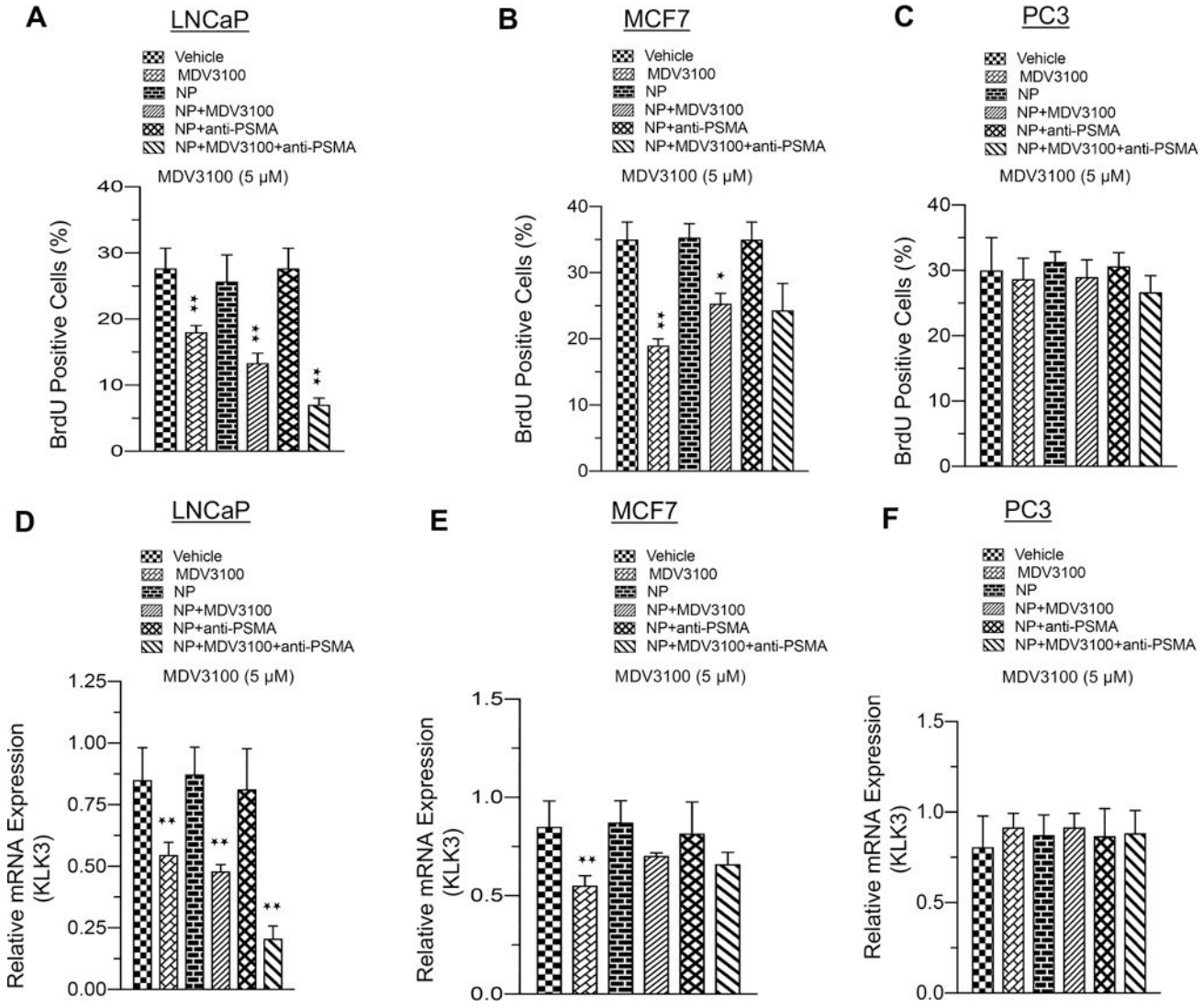

Figure 5.

Enzalutamide-encapsulated–anti-PSMA conjugates of hybrid nanoparticles efficiently control cell cycle and repress AR target gene expression. (A–C) Graphic representation of BrdU analysis in LNCaP, MCF7, and PC3 cells in response to vehicle, enzalutamide, NP, NP +MDV3100, enzalutamide-loaded nanoparticle, nanoparticle with anti-PSMA, or enzalutamide-loaded nanoparticle coated with anti-PSMA. (D–F) Graphic representation of KLK3 mRNA (PSA) analysis in LNCaP, MCF7, and PC3 cells exposed to vehicle, enzalutamide, NP, NP+MDV3100, enzalutamide-loaded nanoparticle, nanoparticle with anti-PSMA, or enzalutamide-loaded nanoparticle coated with anti-PSMA. For these experiments, 5 μM enzalutamide was used. Each data point is a mean ± SD from three or more independent experiments. $^{\star}p$ and $^{\star\star}p < 0.05$ were considered as statistically significant. Note: treated with drugs for 48 h and BrdU pulsed for last 2 h with drug for cell cycle analysis.

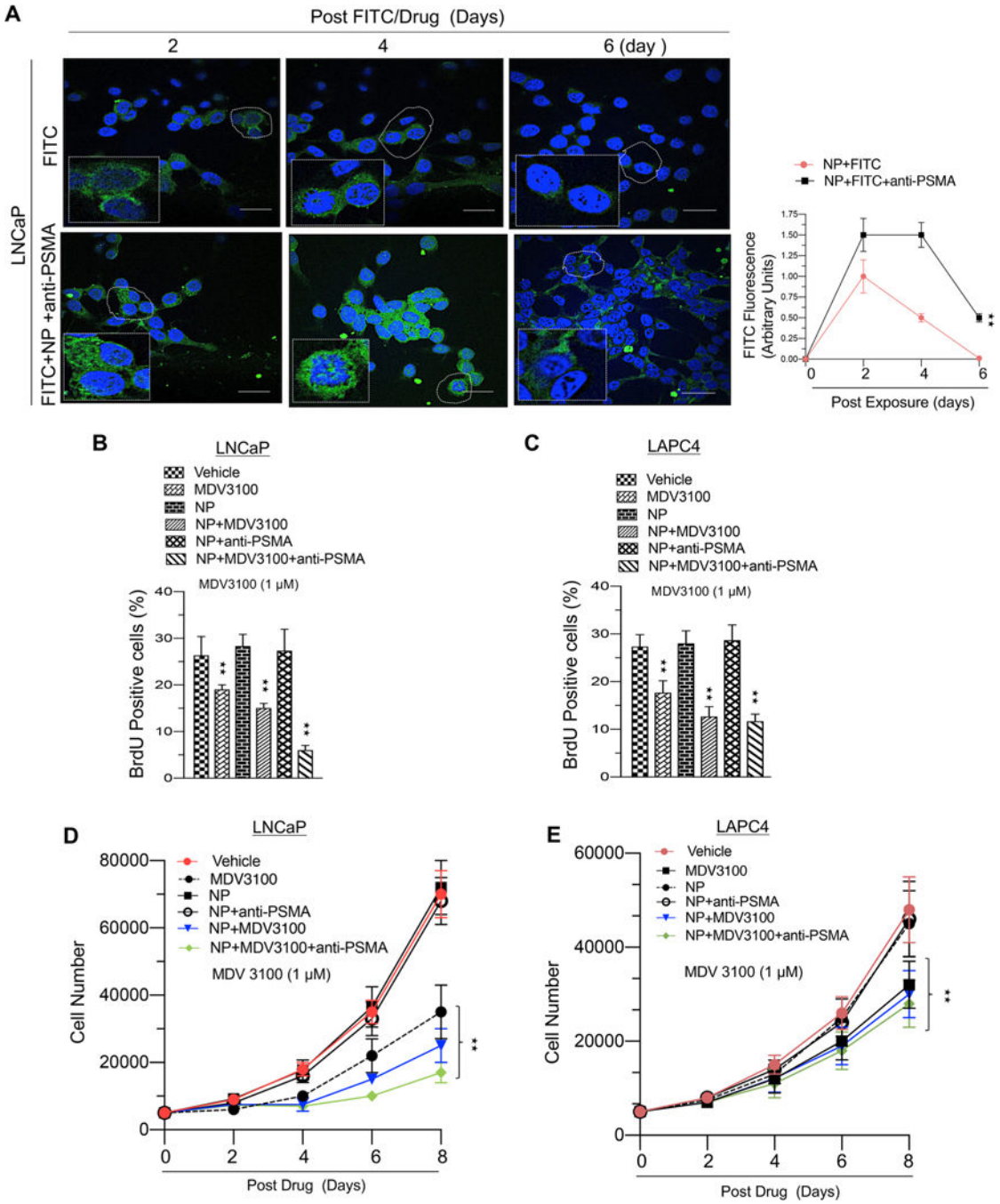

Figure 6.

Lower systemic dose of enzalutamide-encapsulated hybrid nanoparticle–anti-PSMA conjugates enhances therapeutic efficacy in prostate cancer cells. (A) Confocal microscopic images of LNCaP cells exposed to FITC (enzalutamide replaced with FITC) or anti-PSMA conjugates of hybrid nanoparticle-loaded enzalutamide (enzalutamide replaced with FITC) (left panel) exposed for indicated time and a graphic representation of FITC fluorescence (right panel). (B) Graphic representation of BrdU analysis in LNCaP cells in response to vehicle, enzalutamide (1 μM), nanoparticle (NP), NP with enzalutamide (1 μM), NP+PSMA,

or NP+enzalutamide+anti-PSMA (1 μM). (C) Graphic representation of BrdU analysis in LAPC4 cells in response to vehicle, enzalutamide (1 μM), nanoparticle (NP), NP with enzalutamide (1 μM), NP+PSMA, or (NP +enzalutamide+anti-PSMA (1 μM). (D) Graphic representation of cell growth assay in LNCaP cells in response to vehicle, enzalutamide (1 μM), nanoparticle (NP), NP+enzalutamide (1 μM), NP+PSMA, or NP+enzaluamide+anti-PSMA. (E) Graphic representation of BrdU analysis in LAPC4 cells in response to vehicle, enzalutamide (1 μM), nanoparticle (NP), NP+enzalutamide (1 μM), NP+PSMA, or NP +MDV3100+anti-PSMA (1 μM). Each data point is a mean ± SD from three or more independent experiments. ★★$p < 0.05$ were considered as statistically significant.

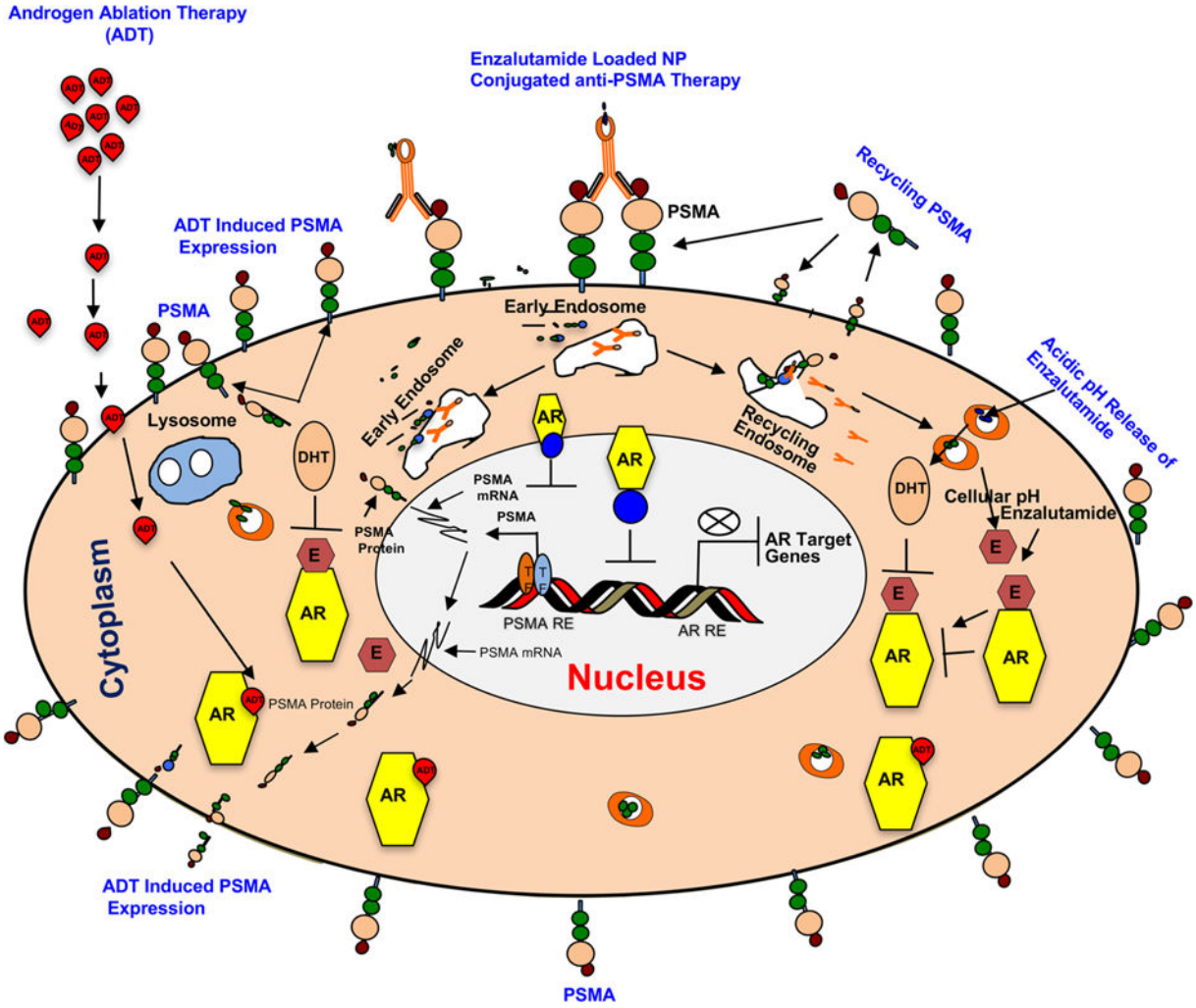

Figure 7.

Working model of enzalutamide-loaded hybrid nanoparticle–anti-PSMA conjugate in PSMA proficient prostate cancer model. Androgen ablation therapy (ADT) increases PSMA expression via activation of PSMA transcription through ADT induced transcription factors (TFs) and PSMA specific internalization of enzalutamide–hybrid nanoparticle–anti-PSMA conjugate and release of enzalutamide inside the cell at a cellular pH (5.0). Cytoplasmic AR bound enzalutamide inhibits the signaling by blocking AR dimerization, blocking AR nuclear translocation, or inhibiting AR association to ARE (Androgen Receptor Response Elements).

Table 1.

Enzalutamide (MDV3100) Encapsulation Efficiency

formula: (amount of drug used – amount of free drug)/amount of drug used × 100		
biological replicate	**values**	**mean (%)**
1	3 mg – 0.8 mg/3 mg × 100 = 73%	
2	3 mg – 0.71 mg/3 mg × 100 = 76.3%	74.8
3	3 mg – 0.75 mg/3 mg × 100 = 75%	

Table 2.

Enzalutamide (MDV3100) Loading Capacity

formula: (amount of drug used – amount of free drug)/total weight of nanoparticles × 100		
biological replicate	**values**	**mean (%)**
1	3 mg – 0.8 mg/7.6 mg × 100 = 28.9%	
2	3 mg – 0.71 mg/7.6 mg × 100 = 30.1%	29.5
3	3 mg – 0.75 mg/7.6 mg × 100 = 29.6%	